Origin of the Spin-Orbital Liquid State in a Nearly $J = 0$ Iridate $Ba_3ZnIr_2O_9$

Abhishek Nag,[1] S. Middey,[2‡] Sayantika Bhowal,[3] S. K. Panda,[2§] Roland Mathieu,[4] J. C. Orain,[5] F. Bert,[5] P. Mendels,[5] P. G. Freeman,[6,7] M. Mansson,[6,8] H. M. Ronnow,[6] M. Telling,[9] P. K. Biswas,[10] D. Sheptyakov,[11] S. D. Kaushik,[12] Vasudeva Siruguri,[12] Carlo Meneghini,[13] D. D. Sarma,[14] Indra Dasgupta,[2,3,*] and Sugata Ray[1,2,†]

[1]*Department of Materials Science, Indian Association for the Cultivation of Science, Jadavpur, Kolkata 700032, India*
[2]*Centre for Advanced Materials, Indian Association for the Cultivation of Science, Jadavpur, Kolkata 700032, India*
[3]*Department of Solid State Physics, Indian Association for the Cultivation of Science, Jadavpur, Kolkata 700032, India*
[4]*Department of Engineering Sciences, Uppsala University, P.O. Box 534, SE-751 21 Uppsala, Sweden*
[5]*Laboratoire de Physique des Solides, UMR CNRS 8502, Université Paris-Sud, 91405 Orsay, France*
[6]*Laboratory for Quantum Magnetism (LQM), École Polytechnique Fédérale de Lausanne (EPFL), Station 3, CH-1015 Lausanne, Switzerland*
[7]*Jeremiah Horrocks Institute for Mathematics, Physics and Astrophysics, University of Central Lancashire, Preston PR1 2HE, United Kingdom*
[8]*Department of Materials and Nanophysics, KTH Royal Institute of Technology, Electrum 229, SE-16440 Kista, Sweden*
[9]*ISIS Facility, Rutherford Appleton Laboratory, Chilton, Didcot, Oxon OX110QX, United Kingdom*
[10]*Laboratory for Muon Spin Spectroscopy, Paul Scherrer Institute, CH-5232 Villigen PSI, Switzerland*
[11]*Laboratory for Neutron Scattering and Imaging, Paul Scherrer Institute, CH-5232 Villigen PSI, Switzerland*
[12]*UGC-DAE-Consortium for Scientific Research Mumbai Centre, R5 Shed, Bhabha Atomic Research Centre, Mumbai 400085, India*
[13]*Dipartimento di Scienze, Universitá Roma Tre, Via della Vasca Navale, 84 I-00146 Roma, Italy*
[14]*Solid State and Structural Chemistry Unit, Indian Institute of Science, Bangalore 560012, India*

(Received 16 July 2015; published 3 March 2016)

We show using detailed magnetic and thermodynamic studies and theoretical calculations that the ground state of $Ba_3ZnIr_2O_9$ is a realization of a novel spin-orbital liquid state. Our results reveal that $Ba_3ZnIr_2O_9$ with Ir^{5+} ($5d^4$) ions and strong spin-orbit coupling (SOC) arrives very close to the elusive $J = 0$ state but each Ir ion still possesses a weak moment. *Ab initio* density functional calculations indicate that this moment is developed due to superexchange, mediated by a strong intradimer hopping mechanism. While the Ir spins within the structural Ir_2O_9 dimer are expected to form a spin-orbit singlet state (SOS) with no resultant moment, substantial frustration arising from interdimer exchange interactions induce quantum fluctuations in these possible SOS states favoring a spin-orbital liquid phase down to at least 100 mK.

DOI: 10.1103/PhysRevLett.116.097205

$5d$ transition metal compounds often exhibit unusual electronic and magnetic properties due to the presence of strong spin-orbit coupling (SOC), comparable to their on-site Coulomb (U) and crystal field (Δ_{CFE}) interactions [1,2]. In the strong spin-orbit coupling regime, M_J ($\sum m_j$) becomes the only valid quantum number instead of m_l (orbital) and m_s (spin), and the multiplets and their degeneracies are solely determined by the total angular momentum J. The electronic and magnetic responses of a system in such limits are not yet well understood and have generated significant curiosity in recent times. For example, the curious insulating state of the layered tetravalent iridates (Ir^{4+}; $5d^5$) has recently been explained within single particle theories assuming splitting of t_{2g} bands into a set of fully filled quartet bands separated from another set of half-filled narrow doublet bands due to finite SOC. The half-filled doublet bands further split into fully occupied lower and empty upper Hubbard bands in the presence of relatively small Hubbard U [3–5].

The pentavalent Iridates (Ir^{5+}; $5d^4$) are more intriguing, where in the strong SOC limit all the spin-orbit entangled electrons will be confined to singlet $J = 0$ ($M_J = 0$) ground state, with no net moment. The evolution of ground and excited states of a low spin $5d$ t_{2g}^4 Ir^{5+} ion as a function of SOC parameter λ' is illustrated in Fig. 1(a) and a $J = 0$ ground state is realized in the strong SOC limit [6]. A possibility of excitonic magnetism has been predicted for these systems where the energy scale of the singlet-triplet splitting determined by SOC is comparable to superexchange interaction promoted by hopping [10]. The breakdown of the $J = 0$ nonmagnetic state in d^4 systems can also be realized within a single electron picture primarily driven by band-structure effect that allows the hybridization between the quartet and the doublet redistributed orbitals (eigenstates of the spin-orbit coupled Hamiltonian). Overall, d^4 Ir compounds in the strong SOC limit may host weak magnetic moment unless the λ' becomes so large that any excitonic or hopping-assisted magnetism becomes forbidden. As a consequence, there are not prominent experimental observations of a $J = 0$ state, excluding just a speculation for $NaIrO_3$ [11]. For example, a recent study [12] on a d^4 system Sr_2YIrO_6 revealed the presence of long range

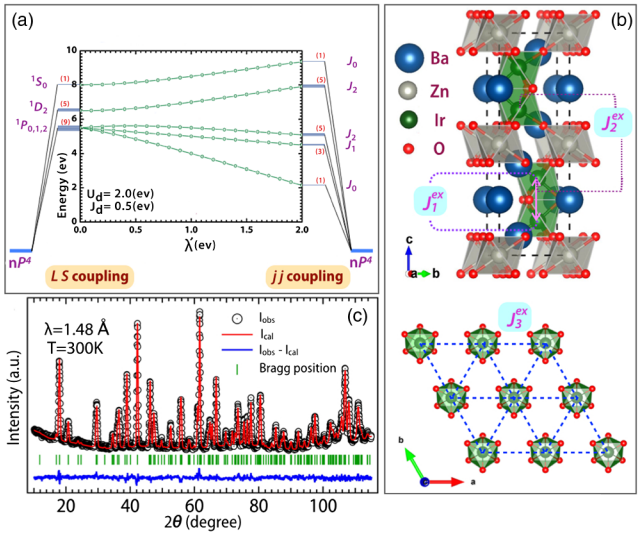

FIG. 1. (a) The energy states of the low spin $5d$ t_{2g}^4 Ir^{5+} ion calculated as a function of SOC. (b) The crystal structure of $Ba_3ZnIr_2O_9$ and the triangular lattice formed by Ir ions in the a-b plane (lower panel). (c) Experimental and refined NPD patterns [13].

magnetic order with a comparatively larger paramagnetic moment of $0.91\mu_B$/Ir (ideal spin-only moment $= 2.83\mu_B$) appearing due to a noncubic IrO_6 crystal field.

Here, we have explored the complex electronic and magnetic interplay of Ir^{5+} within a $6H$ hexagonal compound, namely, $Ba_3ZnIr_2O_9$ (BZIO) [Fig. 1(b)], where the octahedral IrO_6 units share face and form Ir_2O_9 dimers. Our experiments reveal that $Ba_3ZnIr_2O_9$ comes closest to the coveted $J = 0$ ground state but still with low magnetic moments on individual Ir's in the paramagnetic regime. Our density functional calculations reveal that these tiny moments on adjacent Ir sites within a dimer [14] interact antiferromagnetically in the presence of strong spin-orbit coupling and form a nonmagnetic spin-orbital singlet (SOS) state. However, all the experimental studies including detailed muon spin-rotation (μSR), heat capacity, and magnetization measurements, reveal persisting quantum fluctuations down to 100 mK. These fluctuations seem to appear due to comparable *interdimer* hoppings, and geometric frustrations arising from triangular lattice in the a-b plane [Fig. 1(b), lower panel], which destabilizes the SOS state, making it a rare example of a quantum spin-orbital liquid (QSOL) [15].

Polycrystalline $Ba_3ZnIr_2O_9$ (BZIO) was synthesized by standard solid state reaction using stoichiometric amounts of $BaCO_3$, ZnO, and Ir metal as starting materials [16]. First, neutron powder diffraction (NPD) [Fig. 1(c)] recorded at 300 K was satisfactorily refined with space group $P6_3/mmc$ and considering only $< 5\%$ Zn-Ir site disorder; i.e., in more than 95% of cases Ir ions form Ir_2O_9 dimer ($4f$ sites), while Zn ions occupy the isolated octahedral sites ($2a$) sharing corners with the Ir_2O_9 dimers. The structural parameters obtained from the refinement of 1.5 K NPD data (see later), very similar to the 300 K results, are listed in Table I of the Supplemental Material [6]. The local structure obtained (Table I) by x-ray absorption fine structure (XAFS) analysis [17] of Zn K and Ir L_3 edges also confirmed negligible Zn-Ir chemical disorder.

The absence of density of states (DOS) at the Fermi level in valence band photoemission spectra [Fig. 2(a)], discloses a gapped electronic structure in BZIO (also seen in electrical resistivity [6]). This peculiar insulating behavior of Ir^{5+} (confirmed by XPS [6]) was investigated within the single particle mean-field framework using density functional theory (DFT) within the generalized gradient approximation (GGA) [18] and projector augmented wave (PAW) [19–22] calculations by systematically including Hubbard U and SOC (see the Supplemental Material [6] for details). The nonspin polarized DOS of BZIO within GGA is shown in Fig. 2(b). As expected, the system turned out to be metallic with the Fermi level located at the t_{2g} manifold separated from the e_g orbitals by a large octahedral crystal field (~3.5 eV). The DOS is, however, remarkably different upon inclusion of SOC and a Hubbard U ($U_{eff} = 2.5$ eV), which makes the system insulating with a gap of 10 meV [see Fig 2(c) and inset]. In the presence of SOC the t_{2g} orbitals (six orbitals including spin degeneracy) split into twofold degenerate Γ_7 and fourfold degenerate Γ_8 orbitals. Since four electrons are available per Ir, all the Γ_8 orbitals are occupied and the system is insulating as seen experimentally. While analyzing the magnetic properties of $Ba_3ZnIr_2O_9$ in the framework of

TABLE I. Main structural parameters obtained from the multishell fitting of the Zn K-edge and Ir L_3-edge XAFS spectra. The crystallographic distances, as obtained by NPD Rietveld refinement, are reported for sake of comparison. The number in square brackets denote powers of 10.

		Zn K					Ir L_3		
Shell	N	R (Å)	σ^2 (Å^2)	R_{NPD} (Å)	Shell	N	R (Å)	σ^2 (Å^2)	R_{NPD} (Å)
Zn-O	6	2.05(1)	6[−3]	2.08	Ir-O	6	1.96(1)	5.4[−3]	1.9–2.0
					Ir-Ir	1	2.77(2)	4.1[−3]	2.75
Zn-Ba	8	3.55(2)	9.0[−3]	3.58	Ir-Ba	7	3.44(2)	1.4[−2]	3.52
Zn-Ir	6	3.98(4)	1.0[−2]	4.00	Ir-Zn	3	4.01(4)	1.2[−2]	4.00

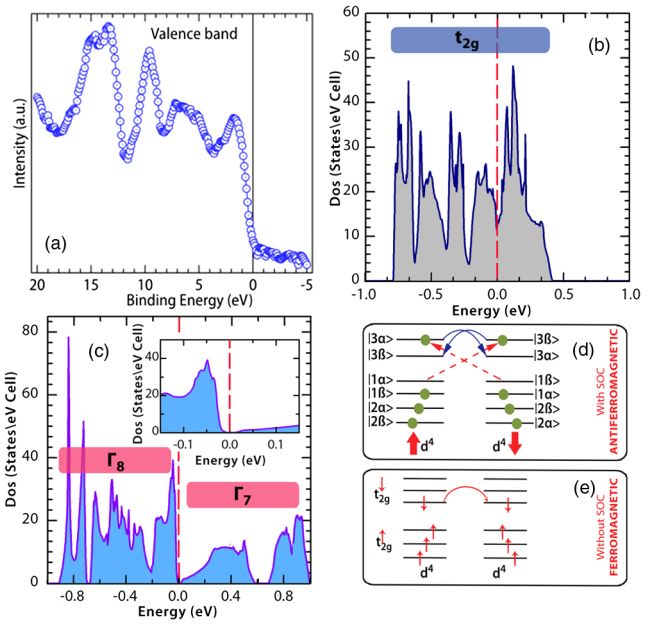

FIG. 2. (a) Valence band photoemission spectra of BZIO. Total DOS obtained within (b) GGA and (c) GGA + SOC+ U. Interaction mechanism in the (d) presence and (e) absence of SOC.

GGA + U + SOC calculations we find that local moments are spontaneously generated in the magnetic phase due to the hybridization between the occupied Γ_8 and empty Γ_7 orbitals of two antiferromagnetic Ir ions within the dimer. In the following, we shall argue that this antiferromagnetic superexchange within the dimer will promote a spin-orbital singlet state. The four Γ_8 orbitals are designated as $|1\alpha\rangle$, $|1\beta\rangle$, $|2\alpha\rangle$, $|2\beta\rangle$ while the two Γ_7 orbitals as $|3\alpha\rangle$, $|3\beta\rangle$ as illustrated in Fig. 2(d). We regard these spin-orbit entangled orbitals as pseudospin orbitals, i.e., the orbital in which one electron occupying $|i\alpha\rangle$ ($|i\beta\rangle$) is considered as up (down) pseudospin. However, unlike t_{2g} orbitals the hopping between these pseudospin orbitals is not always pseudospin conserved [23]. In particular, an electron in a pseudospin orbital $|1\alpha\rangle$ ($|1\beta\rangle$) can hop only to pseudospin orbitals $|j\beta\rangle$ ($|j\alpha\rangle$), where $j \neq 1$ and all other hoppings are pseudospin conserved [23]. Such hopping leads to antiferromagnetic pseudospin interaction within the Ir_2O_9 dimer and thereby favors the SOS state as shown schematically in Fig. 2(d). For an antiferromagnetic configuration of pseudospins in a dimer the Γ_8 electron in the state $|1\alpha\rangle$ and $|1\beta\rangle$ can virtually hop to $|3\beta\rangle$ and $|3\alpha\rangle$, respectively, as this hopping is not pseudospin conserved [indicated by ⇢ in Fig. 2(d)]. Once these electrons are promoted to the Γ_7 orbitals, they can then gain energy by hopping to the other Γ_7 orbital, as this hopping is now pseudospin conserved [indicated by → in Fig. 2(d)]. This latter hopping is, however, not possible if the pseudospins residing in the dimer were parallel. The same dimer, however, favors ferromagnetic interaction in the absence of SOC as illustrated in Fig. 2(e) as the hopping between the t_{2g} orbitals are spin conserved. In order to check the above mentioned scenarios, we carried out spin polarized GGA + U and GGA + U + SOC calculations for several magnetic configurations [6]. The GGA + U + SOC calculations reveal a rather large spin moment [$(0.65–0.75)\mu_B$] per Ir atom confirming our model. In addition, the large value of the orbital moment ($0.26\,\mu_B$) confirms the importance of SOC. Although this lowest energy antiferromagnetic intradimer coupling (SOS) is expected to give rise to a long-range spin-gap state, substantial interdimer exchange ($J_3^{ex} = -1.5$ meV with 6 neighbors in the a-b plane and $J_2^{ex} = -1.6$ meV with 3 neighbors $\perp a$-b plane) compared to the intradimer exchange ($J_1^{ex} = -14.6$ meV) induces frustration in the system.

Such a degree of frustration is preliminarily confirmed by NPD at 1.5 K [Fig. 3(a)] whose refinement shows no ordered moment down to 1.5 K within the detection limit ($0.5\mu_B$). In order to further probe the character of this frustration driven magnetic disorder, next we studied μSR in zero field, a technique perfectly suited to detect weak and/or partial freezing of local magnetic moments. The evolution of muon polarization in the sample is shown in Fig. 3(b). At high temperature, the slow Gaussian-like relaxation arises from nuclear dipoles which are static in the μSR time window and gives a T independent contribution. Upon lowering temperature, the relaxation rate increases gradually from about 100 K as a result of slowing down of the electronic fluctuations and strikingly levels off below about 2 K as demonstrated by the nearly perfect overlap of the 2 and 0.1 K polarization curves. Despite this obvious slowing down of the dynamics, we did not observe any spontaneous oscillations or emergence of a "1/3rd" tail that would signal a magnetic transition to a frozen state.

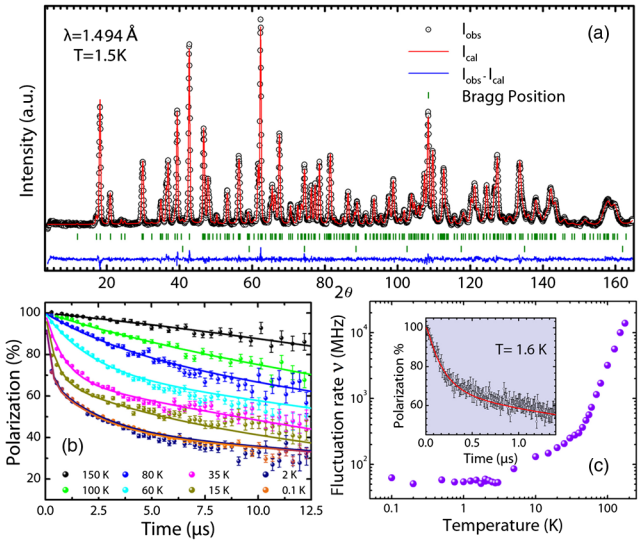

FIG. 3. (a) High resolution NPD recorded at 1.5 K. (b) Time evolution of muon polarization in $Ba_3ZnIr_2O_9$ in zero external field at different temperatures. (c) Fluctuation rate of the internal fields vs temperature. Inset: The fast initial relaxation of the muon polarization at low temperature.

The robustness of the relaxation to the application of a longitudinal field at base temperature also supports its dynamical origin [6]. Therefore, it can be concluded that the system does not order while the spins continue to fluctuate down to 0.1 K at least. In the low temperature regime, below about 35 K, the signal appears to be composed of at least 3 components—one fast relaxing, one with a moderate relaxation rate, and one hardly relaxing. The data was fitted to the model,

$$P(t) = f_{\text{fast}} G(t, \Delta H_1, \nu) + f_{\text{slow}} G(t, \Delta H_2, \nu) + (1 - f_{\text{fast}} - f_{\text{slow}}) \text{KT}(t, \Delta H), \quad (1)$$

where KT is the Kubo-Toyabe function [24] accounting for the static nuclear field distribution of width ΔH, f_{fast} and f_{slow} are the fractions of the two more relaxing components, and $G(t, \Delta H, \nu)$ is the dynamical relaxation function introduced in Ref. [25] to account for the effect of a fluctuating field distribution of width ΔH at a rate ν. The fits with respect to this model are shown in Fig. 3(b), where only the fluctuation rate ν was allowed to vary with temperature and the extracted values are given in Fig. 3(c). At the lowest measured temperatures we note that for both relaxing components the inequality $\nu > \gamma \Delta H$, where $\gamma = 2\pi \times 135.5$ Mrad s^{-1} T^{-1} is the muon gyromagnetic ratio, still holds since $\gamma \Delta H_1 = 12.5$ and $\gamma \Delta H_2 = 3.4$ μs^{-1} [Fig. 3(c)]. This validates the use of dynamical relaxation functions, in line with the absence of usual evidence for a frozen ground state. The above prediction of a special QSOL state in BZIO is further confirmed by the analysis of heat capacity (C). The temperature variation of C [Fig. 4(a)] does not show any peak or anomaly, consistent with the absence of any structural and/or long range magnetic transition. To extract the magnetic heat capacity C_m by subtracting the lattice contribution, C was also measured for isostructural nonmagnetic $Ba_3ZnSb_2O_9$. The difference of molecular weight between these two compounds has been taken into account following the scaling procedure by Bouvier *et al.* [26]. The obtained C_m is plotted in Fig. 4(b), which shows only a broad peak around ~15 K followed by a decay around 30 K. A fit of the magnetic heat capacity ($C_m = \gamma T + \beta T^2$) at a comparatively higher temperature range (3–9 K) roughly gives a strong T-linear contribution of $\gamma = 25.9$ mJ/mol K^2, unusual for insulating systems. Also, the finite γ value does not change with application of external magnetic field as high as 90 kOe, suggesting its origin to be gapless excitations from spinon density of the QSOL state or minor lattice oxygen vacancies, but not any paramagnetic impurity [27–31], as seen in other spin liquid systems too [32–35]. The magnetic entropy obtained by integrating C_m/T with T is shown in Fig. 4(c), which is negligible (~7%) if one considers spin-only magnetic entropy, $R \ln(2J + 1)$ with $S = 1$, unlike other spin liquid candidates containing $3d$ TM [32,33,36]. On the other hand, the magnetic entropy is expected to be 0 for a spin-orbit coupled magnetic entropy, $R \ln(2J + 1)$ with $J = 0$, and the present system seems very close to that. Therefore, the heat capacity study affirms the presence of a QSOL-like dynamical ground state with weak Ir moments, visible below 30 K, and negates the presence of paramagnetism that might arise from Zn-Ir site disorder or other defects.

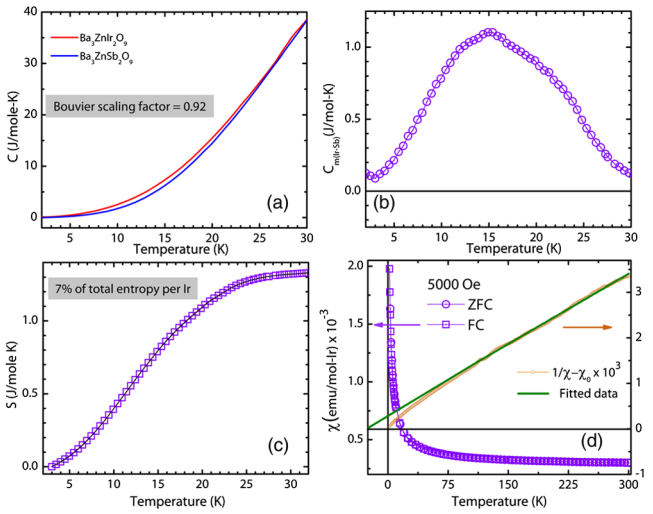

FIG. 4. Temperature dependence of (a) specific heat (C), (b) magnetic specific heat (C_m) capacity after subtracting the lattice contribution, and (c) magnetic entropy. (d) FC-ZFC magnetization measured at 5000 Oe magnetic field fitted using the Curie-Weiss law.

Finally, we show the temperature dependence of field-cooled and zero-field-cooled magnetization measured with 5000 Oe field in Fig. 4(d). These χ vs T curves are fitted with $\chi_0 + C_W/(T - \Theta_W)$, where χ_0 is the temperature independent paramagnetic susceptibility, C_W and Θ_W represent the Curie constant and Curie-Weiss temperature, respectively, and the result is shown as a green straight line, laid on the $1/(\chi - \chi_0)$ vs T data. The fitting, especially at the higher temperature region, extracts a Θ_W value ~ -30 K and a moment of $\sim 0.2 \mu_B$/Ir. The reasonably large value of $\Theta_W = -30$ K in the absence of any magnetic ordering down to at least 100 mK further proves that the system indeed behaves like a QSOL.

In conclusion, we find BZIO is a close realization of a $J = 0$ insulator where the origin of the small nonzero moment is the superexchange induced spin excitations within two Ir ions of the Ir_2O_9 dimer maintaining an antiferromagnetic orientation. However, strong interdimer hoppings in the $a - b$ plane induce quantum fluctuations and a long-range SOS-like magnetic order is suppressed due to geometric frustration, resulting in a quantum spin-orbital liquid state, confirmed both by μSR and heat capacity studies.

A. N. and S. B. thank Council of Scientific & Industrial Research (CSIR), India for support. S. R. thanks CSIR,

India for funding [Project No. (1269)/13/EMR-II], Department of Science and Technology Indo-Italian POC for experiments at Elettra, and Saha Institute of Nuclear Physics, India for facilitating the experiments at the Indian Beamline, Photon Factory, KEK, Japan. M. M. was supported by Marie Skłodowska Curie Action, International Career Grant through the European Commission and Swedish Research Council (VR), Grant No. INCA-2014-6426. J. C. O., F. B., and P. M. thank the French Agence Nationale de la Recherche for its funding (Grant "SPINLIQ" No. ANR-12-BS04-0021). NPD measurements presented in this manuscript are partially based on experiments performed at the Swiss spallation neutron source SINQ, Paul Scherrer Institute, Villigen, Switzerland. We thank the Indo-Swiss Joint Research Programme, Swiss National Science Foundation, and its Sinergia network Mott Physics Beyond the Heisenberg Model (MPBH). We thank Professor Khaliullin and Professor Mahajan for useful discussion.

A. N. and S. M. contributed equally to this work.

*sspid@iacs.res.in
†mssr@iacs.res.in
‡Present address: Department of Physics, University of Arkansas, Fayetteville, Arkansas 72701, USA.
§Present address: Uppsala University, Uppsala, Sweden.

[1] W. Witczak-Krempa, G. Chen, Y. B. Kim, and L. Balents, Annu. Rev. Condens. Matter Phys. **5**, 57 (2014).
[2] J. G. Rau, E. K.-H. Lee, and H.-Y. Kee, arXiv: 1507.06323v1 [Annu. Rev. Condens. Matter Phys. (to be published)].
[3] B. J. Kim *et al.*, Phys. Rev. Lett. **101**, 076402 (2008).
[4] S. J. Moon *et al.*, Phys. Rev. Lett. **101**, 226402 (2008).
[5] B. J. Kim, H. Ohsumi, T. Komesu, S. Sakai, T. Morita, H. Takagi, and T. Arima, Science **323**, 1329 (2009).
[6] See Supplemental Material at http://link.aps.org/supplemental/10.1103/PhysRevLett.116.097205, which includes Ref. [7–9] and derivation of the energy level diagram for t_{2g}^4 configuration in the *L-S* and *j-j* coupling scheme, experimental and theoretical methods, structural parameters obtained from Rietveld refinement of the NPD spectrum of $Ba_3ZnIr_2O_9$ at 1.5 K, electrical resistivity data, photoelectron spectra of Ir 4*f* core level, density functional theory calculations, pseudospin orbitals, results of spin-polarized calculations, and the effect of magnetic field on muon spin rotation (μSR).
[7] J. Rodríguez-Carvajal, Physica B (Amsterdam) **192**, 55 (1993).
[8] T. Otsubo, S. Takase, and Y. Shimizu, ECS Trans. **3**, 263 (2006).
[9] V. I. Anisimov, J. Zaanen, and O. K. Andersen, Phys. Rev. B **44**, 943 (1991).
[10] G. Khaliullin, Phys. Rev. Lett. **111**, 197201 (2013).
[11] M. Bremholm, S. E. Dutton, P. W. Stephens, and R. J. Cava, J. Solid State Chem. **184**, 601 (2011).
[12] G. Cao, T. F. Qi, L. Li, J. Terzic, S. J. Yuan, L. E. DeLong, G. Murthy, and R. K. Kaul, Phys. Rev. Lett. **112**, 056402 (2014).
[13] K. Momma and F.Izumi, J. Appl. Crystallogr. **44**, 1272 (2011).
[14] A. N. Vasilev, M. M. Markina, and E. A. Popova, Low Temp. Phys. **31**, 203 (2005).
[15] G. Chen, L. Balents, and A. P. Schnyder, Phys. Rev. Lett. **102**, 096406 (2009).
[16] T. Sakamoto, Y. Doi, and Y. Hinatsu, J. Solid State Chem. **179**, 2595 (2006).
[17] S. Middey, S. Ray, K. Mukherjee, P. L. Paulose, E. V. Sampathkumaran, C. Meneghini, S. D. Kaushik, V. Siruguri, K. Kovnir, and D. D. Sarma, Phys. Rev. B **83**, 144419 (2011).
[18] J. P. Perdew, K. Burke, and M. Ernzerhof, Phys. Rev. Lett. **77**, 3865 (1996).
[19] G. Kresse and J. Hafner, Phys. Rev. B **47**, 558 (1993).
[20] G. Kresse and J. Furthmüller, Phys. Rev. B **54**, 11169 (1996).
[21] P. E. Blöchl, Phys. Rev. B **50**, 17953 (1994).
[22] G. Kresse and D. Joubert, Phys. Rev. B **59**, 1758 (1999).
[23] H. Matsuura and M. Ogata, J. Phys. Soc. Jpn. **83**, 093701 (2014).
[24] R. S. Hayano, Y. J. Uemura, J. Imazato, N. Nishida, T. Yamazaki, and R. Kubo, Phys. Rev. B **20**, 850 (1979).
[25] A. Keren, Phys. Rev. B **50**, 10039 (1994).
[26] M. Bouvier, P. Lethuillier, and D. Schmitt, Phys. Rev. B **43**, 13137 (1991).
[27] T. H. Han, R. Chisnell, C. J. Bonnoit, D. E. Freedman, V. S. Zapf, N. Harrison, D. G. Nocera, Y. Takano, and Y. S. Lee, arXiv:1402.2693.
[28] L. Clark *et al.*, Phys. Rev. Lett. **110**, 207208 (2013).
[29] S. Yamashita, T. Yamamoto, Y. Nakazawa, M. Tamura, and R. Kato, Nat. Commun. **2**, 275 (2011).
[30] S. Yamashita, Y. Nakazawa, M. Oguni, Y. Oshima, H. Nojiri, Y. Shimizu, K. Miyagawa, and K. Kanoda, Nat. Phys. **4**, 459 (2008).
[31] J. M. Schliesser and B. F. Woodfield, Phys. Rev. B **91**, 024109 (2015).
[32] H. D. Zhou, E. S. Choi, G. Li, L. Balicas, C. R. Wiebe, Y. Qiu, J. R. D. Copley, and J. S. Gardner, Phys. Rev. Lett. **106**, 147204 (2011).
[33] J. G. Cheng, G. Li, L. Balicas, J. S. Zhou, J. B. Goodenough, C. Xu, and H. D. Zhou, Phys. Rev. Lett. **107**, 197204 (2011).
[34] S. Nakatsuji *et al.*, Science **309**, 1697 (2005).
[35] T. Dey, A. V. Mahajan, P. Khuntia, M. Baenitz, B. Koteswararao, and F. C. Chou, Phys. Rev. B **86**, 140405 (R) (2012).
[36] A. P. Ramirez, B. Hessen, and M. Winklemann, Phys. Rev. Lett. **84**, 2957 (2000).